



## High-purity Polypropylene from Disposable Face Masks via Solvent-Targeted Recovery and Precipitation

Journal:	<i>Green Chemistry</i>
Manuscript ID	GC-ART-01-2023-000205.R2
Article Type:	Paper
Date Submitted by the Author:	17-May-2023
Complete List of Authors:	<p>Yu, Jiuling; University of Wisconsin-Madison, Department of Chemical and Biological Engineering  Munguía-López, Aurora del Carmen; University of Wisconsin-Madison, Department of Chemical and Biological Engineering  Cecon, Victor; Iowa State University, Department of Food Science and Human Nutrition  Sánchez-Rivera, Kevin; University of Wisconsin-Madison, Chemical and Biological Engineering  Nelson, Kevin; Amcor Flexibles Neenah Innovation Center  Wu, Jiayang; University of Wisconsin, Chemical and Biological Engineering;  Kolapkar, Shreyas; Michigan Technological University  Zavala, Victor; University of Wisconsin-Madison, Chemical and Biological Engineering  Curtzwiler, Greg; Iowa State University of Science and Technology, Polymer and Food Protection Consortium; Iowa State University of Science and Technology, Food Science and Human Nutrition  Vorst, Keith; Iowa State Univ  Bar-Ziv, Ezra; Michigan Technological University  Huber, George; University of Wisconsin, Chemical and Biological Engineering</p>

# High-purity Polypropylene from Disposable Face Masks via Solvent-Targeted Recovery and Precipitation

Jiuling Yu<sup>a</sup>, Aurora del Carmen Munguía-López<sup>a</sup>, Victor S. Cecon<sup>b,c</sup>, Kevin L. Sánchez-Rivera<sup>a</sup>, Kevin Nelson<sup>d</sup>, Jiayang Wu<sup>a</sup>, Shreyas Kolapkar<sup>e</sup>, Victor M. Zavala<sup>a</sup>, Greg W. Curtzwiler<sup>b,c</sup>, Keith L. Vorst<sup>b,c</sup>, Ezra Bar-Ziv<sup>e</sup>, George W. Huber<sup>a\*</sup>

<sup>a</sup> Department of Chemical and Biological Engineering, University of Wisconsin-Madison, Madison, WI, 53706, USA

<sup>b</sup> Polymer and Food Protection Consortium, Iowa State University, Ames, IA, 50011, USA

<sup>c</sup> Department of Food Science and Human Nutrition, Iowa State University, Ames, IA, 50011, USA

<sup>d</sup> Amcor, Neenah Innovation Center, Neenah, WI, 54956, USA

<sup>e</sup> Mechanical Engineering - Engineering Mechanics, Michigan Technological University, Houghton, MI, 49931, USA

## Abstract

The high use of disposable face masks since the start of COVID-19 has globally generated 4.68-6.24 million tons per year of waste from personal protective equipment. Disposable face masks are generally disposed of in landfills. Polypropylene (PP) is the main component in face masks, which is one of the least recycled plastics but has a high market value. In this work, we extract high-quality PP from face masks using solvent-targeted recovery and precipitation (STRAP) with 90 wt-% recovery. N,N-Dimethylacetamide removed the color from the recovered PP to produce a clear high-purity PP, as verified by CIELAB color space. The decolored PP shows similar thermochemical properties and color to virgin PP resin. A techno-economic analysis of the process indicates that high-purity PP recovery can be economically viable at a scale of 5,000 tons per year or higher.

## Keywords

Polypropylene recycling

Disposable face mask

STRAP

Decolorization

## 1. Introduction

The global pandemic of Coronavirus disease 2019 (COVID-19) has increased the use of disposable face masks with an estimated monthly consumption of 129 billion masks, which weigh 0.39-0.52 million tons.<sup>1-3</sup> Disposable face masks typically contain five components: outer layer, middle layer, inner layer, ear loop, and nose support. The outer and inner layers are typically made of spun bond non-woven polypropylene (PP) fabric, and the middle layer consists of melt blown non-woven PP fabric.<sup>4</sup> The outer PP is typically dyed blue. Ear loops use different polymers including nylon<sup>5</sup>, polyurethane<sup>4</sup>, and polyethylene terephthalate (PET)<sup>6</sup> depending on the manufacturer. The nose support could be made of PP resin with or without metal wire. Lacking effective recycling techniques for disposable face masks, the ultimate destination of masks is either landfills or combustion in incineration facilities.<sup>7</sup>

Face masks cannot be recycled using mechanical recycling because they are a mixture of different polymer materials. A handful of approaches have been reported to try and recycle face masks. Jung et al. studied the catalytic pyrolysis of face masks to produce syngas and C<sub>1-2</sub> hydrocarbons.<sup>5</sup> Yu et al. studied a method to fabricate carbon nanotubes (CNTs)/Ni hybrids via catalytic carbonization from face masks with microwave absorption.<sup>8</sup> It would be desirable to produce higher quality materials from used face masks. Recently, our group has reported a novel route, named solvent-targeted recovery and precipitation (STRAP), that uses solvents to selectively dissolve and precipitate a polymer from polymer mixtures. We have demonstrated this approach with multilayer plastic films under relatively mild conditions.<sup>9, 10</sup> However, we have not reported any work on the recovery of polymers from fabrics or textiles. To validate the feasibility of STRAP on different feedstocks and polymers, in this paper, we show that PP could be efficiently recovered from face masks using STRAP method, especially without pre-separation of ear loop and nose support. The recovered PP could be upgraded to high-purity PP by a simple decolorization step. This study is a step forward on recycling face mask to PP, as well as minimizing its environmental pollution generated from landfills or combustion.

## 2. Methods

### 2.1 Materials

New disposable protective face masks (new masks) were purchased (T·IMTEX, Zhongshan Timtex Industrial Co., Ltd, China). Used face masks (used masks) were collected from the TerraCycle Zero Waste Box™ (for Disposable Masks) in the lobby of Engineering Hall at the University of Wisconsin-Madison and stored for 2 months to kill any potential viruses. The entire new and used face masks, including ear loop and nose support, were shredded twice through a 1/8" cross-cut shredder (Allegheny 16-75CX) at Michigan Technological University. Polypropylene (isotactic, average Mw ~12,000 Da, average Mn ~5,000 Da), toluene (ACS reagent, ≥99.5%), N,N-

Dimethylacetamide (DMAc, ReagentPlus®, ≥99%), 2,6-di-tert-butyl-4-methylphenol (BHT, ≥99.0%), 1,1,2,2-tetrachloroethane-*d*<sub>2</sub> (deuteration degree ≥99.5% for NMR spectroscopy) were ordered from Sigma-Aldrich (St. Louis, Missouri, USA) and used as received. HPLC grade 1,2,4-trichlorobenzene (TCB) and HPLC grade methanol were ordered from Fisher Scientific (Fair Lawn, New Jersey, USA).

## 2.2 Experimental procedure

### 2.2.1 Polymer extraction via STRAP process

Figure 1 shows the three steps for recycling face masks: (A) 5 g new or used masks were added into 75 g toluene solvent (mask : toluene mass ratio = 1:15) at targeted temperature  $T$  ( $T=90^{\circ}\text{C}$ ,  $100^{\circ}\text{C}$ , and  $110^{\circ}\text{C}$ ) for different dissolution time  $t$  ( $t=5$  min, 10 min, 30 min, and 60 min) with magnetic stirring; (B) the solvent was separated from the undissolved polymer using a stainless wire cloth (opening size 0.0277-inch, open area 44.2%); (C) the temperature was reduced to  $60^{\circ}\text{C}$  and the polymer was precipitated. The precipitated polymer component was filtered mechanically under vacuum. The recovered polymer was then dried in a vacuum oven at  $75^{\circ}\text{C}$  for 2 hrs. The yields at different temperatures and dissolution times were plotted in Figures S1-2. The solubility of virgin PP (from Sigma-Aldrich) in toluene at  $110^{\circ}\text{C}$  is 31.2 wt-% (g solute/100 g solution).<sup>11</sup> This process was able to extract 3.6 g of PP from 5 g of used face masks in toluene at  $110^{\circ}\text{C}$ .

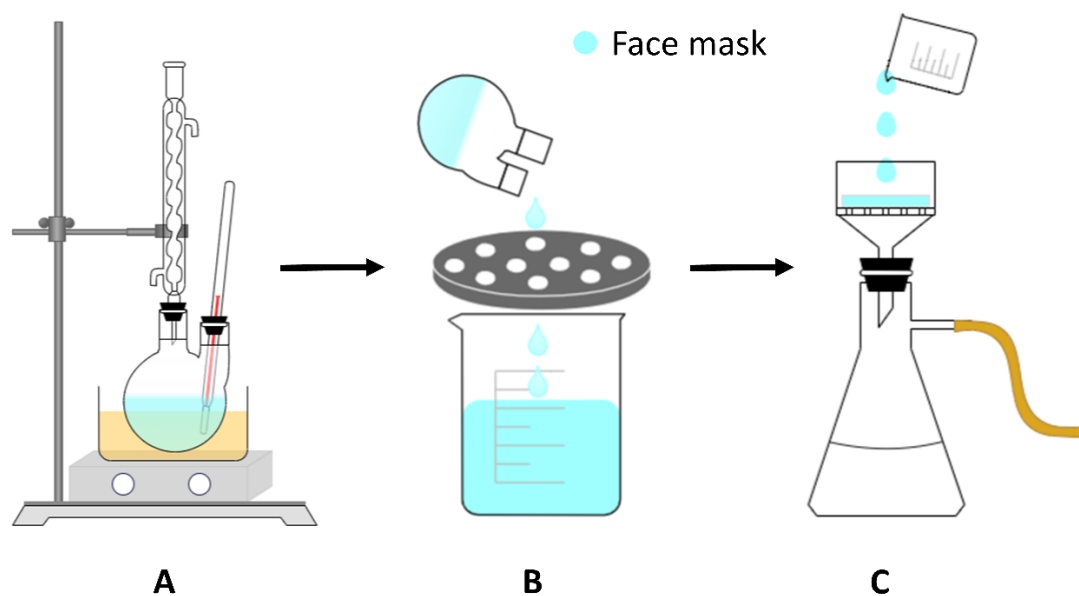


Figure 1. Schematic diagram of workflow for face mask recycling.

### 2.2.2 Decolorization process

Extracted PP from STRAP process had a light blue color after drying. A subsequent decolorization step was applied to the extracted polymers. The extracted PP clumped

together in particle sizes of approximately 20-70 mm. These clumps were ground to 3 mm before color removal to increase the surface area and accelerate the decolorization rate. 4 g ground PP was added to 60 g pre-heated DMAc (ground PP: DMAc mass ratio = 1:15) at 115°C for 5 min or 60 min. Next, decolored PP was filtered from DMAc and dried at 100°C for 2 hrs in a vacuum oven. After drying, the yield of decolored PP ranged in 94-98 wt-%.

### 2.3 Statistical analysis

The yield results were expressed as means  $\pm$  standard deviations with three replicate experiments. They were analyzed and statistically examined by one-way analysis of variance (one-way ANOVA) and a Duncan's multiple range test using SPSS version 17.0 software. The PP recovery yield was compared at different conditions and statistical significance was considered at the level of  $P < 0.05$ .<sup>12, 13</sup>

### 2.4 Characterization

Attenuated total reflectance Fourier-transform infrared (ATR-FTIR) spectra were acquired with a Bruker Vertex 70 FTIR spectrometer equipped with a liquid nitrogen-cooled Mercury-Cadmium-Telluride (MCT) detector (Bruker Corporation, Billerica, Massachusetts, USA). An average of 128 scans was collected in the range of 4000-400  $\text{cm}^{-1}$  with a resolution of 4  $\text{cm}^{-1}$ . Each spectrum was scanned with an air background. Thermogravimetric analysis (TGA) was conducted on a TGA Q500 analyzer (TA Instruments, New Castle, Delaware, USA) from 40°C to 600°C with a ramping rate of 10°C/min under a nitrogen flow rate of 50.0 mL/min. Differential scanning calorimetry (DSC) was used to estimate the melting temperature ( $T_m$ ) and crystallization temperature ( $T_c$ ) on a DSC Q100 calorimeter equipped with a Refrigerated Cooling System 90 (TA Instruments, New Castle, Delaware, USA). Samples were encapsulated in standard aluminum pans, heated from 40°C to 280°C with a ramping rate of 10°C/min and cooled from 280°C to 40°C at the same ramping rate. The heating/cooling process was looped twice under a 50.0 mL/min nitrogen flow rate. High Temperature Gel Permeation Chromatography (HT-GPC) was used to determine the molecular weight and molecular weight distribution of the polymers, which was carried out in a Malvern Viscotek 350 HT-GPC (Malvern Panalytical, Westborough, Massachusetts, USA), equipped with an internal filtration system and refractive index (RI), viscometer, and light scattering (LS) detectors. All samples were dissolved in 1,2,4-trichlorobenzene (TCB), containing 250 mg/L of 2,6-di-tert-butyl-4-methylphenol (BHT) as an antioxidant. A flow rate of 1.0 mL/min and an oven temperature of 145°C using two PLgel Olexis 300 x 7.5 mm columns (Agilent Technologies, Santa Clara, California, USA) in series were used for separation. A calibration curve was obtained using narrow polystyrene standards from 10,000 to 3,000,000 Da (Agilent Technologies, Santa Clara, California, USA) and converted for use with polypropylene using Mark-Houwink constants, as described in ASTM D6474-20,<sup>14</sup> with the WinGPC software (PSS USA, Amherst, Massachusetts, USA).

Inductively Coupled Plasma-Optical Emission Spectroscopy (ICP-OES) spectra were analyzed using an iCap-7400 Duo ICP-OES (Thermo Scientific, Waltham, Massachusetts, USA), in order to quantify the content of Al (aluminum), Cr (chromium), Cu (copper), Fe (iron), Ni (nickel), and Ti (titanium). The multi-element standard contained 0.1  $\mu\text{g/mL}$ , 1  $\mu\text{g/mL}$ , 5  $\mu\text{g/mL}$ , 25  $\mu\text{g/mL}$ , 50  $\mu\text{g/mL}$ , and 100  $\mu\text{g/mL}$  of each metal of interest, along with a 5  $\mu\text{g/mL}$  yttrium solution as the internal standard.<sup>15</sup> Color quantification was performed on an X-Rite Color i5 spectrophotometer (X-Rite, Grand Rapids, Michigan, USA) which could convert measurements directly into CIELAB color space nomenclature, referred to as  $L^*a^*b^*$  ( $L^*$  for perceived lightness,  $a^*$  for red-green component and  $b^*$  for blue-yellow component).<sup>16</sup> Nuclear magnetic resonance (NMR) spectra were recorded on a Bruker Avance 500 MHz spectrometer (Bruker Corporation, Billerica, Massachusetts, USA) using a BBFO liquids probe. Approximately 75 mg polymer sample was dissolved in 0.5 mL 1,1,2,2-tetrachloroethane- $d_2$  and 10  $\mu\text{L}$  toluene (internal standard). Data acquisition for obtaining the  $^1\text{H}$  spectrum (zg30) was performed at 120  $^\circ\text{C}$  for 16 scans, with delay and acquisition time of 3 and 3.285 s, respectively. Data acquisition for obtaining the quantitative  $^{13}\text{C}$  spectrum (zqig30) was performed at 120  $^\circ\text{C}$  for 3,600 scans, with delay and acquisition times of 10 and 1 s, respectively. The peaks were assigned according to the literatures.<sup>17-20</sup> The chemical shifts of both  $^1\text{H}$  spectrum and  $^{13}\text{C}$  spectrum were calibrated with the 1,1,2,2-tetrachloroethane- $d_2$  solvent peak: 6.00 ppm for  $^1\text{H}$  spectrum and 74.0 ppm for  $^{13}\text{C}$  spectrum.<sup>21</sup> High performance liquid chromatography (HPLC) was measured by a Waters 2695 separation module equipped with a Luna C18 (Phenomenex, part No. 00G-4041-E0) HPLC column and a Waters 2998 PDA detector (Waters Corporation, Milford, Massachusetts, USA), set at 230 nm for toluene and 250 nm for DMAc. All liquids were filtered with 0.2  $\mu\text{m}$  PTFE filter before injecting into the HPLC and HPLC column temperature was maintained at 50 $^\circ\text{C}$ . The mobile phase was a gradient methanol/water (with 0.1 wt-% formic acid) at a constant flow rate of 1.0 mL/min (0.1 wt-% formic acid water linearly changed to methanol in 20 min, pure methanol for 7 min, and methanol was linearly changed to 0.1% formic acid water in 3 min).<sup>22</sup> Gas chromatography-mass spectrometry (GC-MS) was analyzed on a Shimadzu GCMS-QP2010 mass spectrometer with an RTX-VMS column and quadrupole MS (Shimadzu Corporation, Kyoto, Japan).

## 2.5 Technoeconomic analysis (TEA) and environmental impact analysis

We performed the process design and TEA using the open-source platform BioSTEAM.<sup>23</sup> This Python-based process simulator has been validated against proprietary software (SuperPro Designer and Aspen Plus). The environmental impact on climate change (kg  $\text{CO}_2$  eq.) for STRAP was analyzed using a life cycle assessment (LCA) methodology. The LCA data for solvents and for the virgin production of polypropylene are taken from the Ecoinvent 3.6 cut-off by classification database using the Environmental Footprint method. Data for the STRAP process utilities (steam, electricity, and cooling agents), as well as the transportation of commodities, are taken from the Environmental Footprint database.

### 3. Results and discussion

#### 3.1 Identification of polymer components in face masks

Figure 2a shows the five components of a face mask: outer layer, middle layer, inner layer, nose support, and ear loop. Each part was characterized by ATR-FTIR. The outer, middle and inner layers had similar FTIR spectra with a broad absorption range from 2800 to 3000  $\text{cm}^{-1}$  and two distinct peaks at 1455 and 1376  $\text{cm}^{-1}$  (Figure 2b). These peaks were identical to the characteristic peaks of PP. The nose support was verified to constitute PP without any other polymer component (Figure 2c). Metal scraps were found in the nose supports for the used face masks. Nose supports can be made of metal wire (e.g., Fe) and wrapped by other polymers.<sup>5</sup> The main component of the ear loop was nylon 6 as shown in Figure 2d. The weight percentage of each component was calculated from ten fragments of new face masks, as shown in Figure 2e. PP was the primary component with 81.3 wt-% of the total mass. Here, the weight percentage of the nose support was not included because of compositional variability among manufacturers.

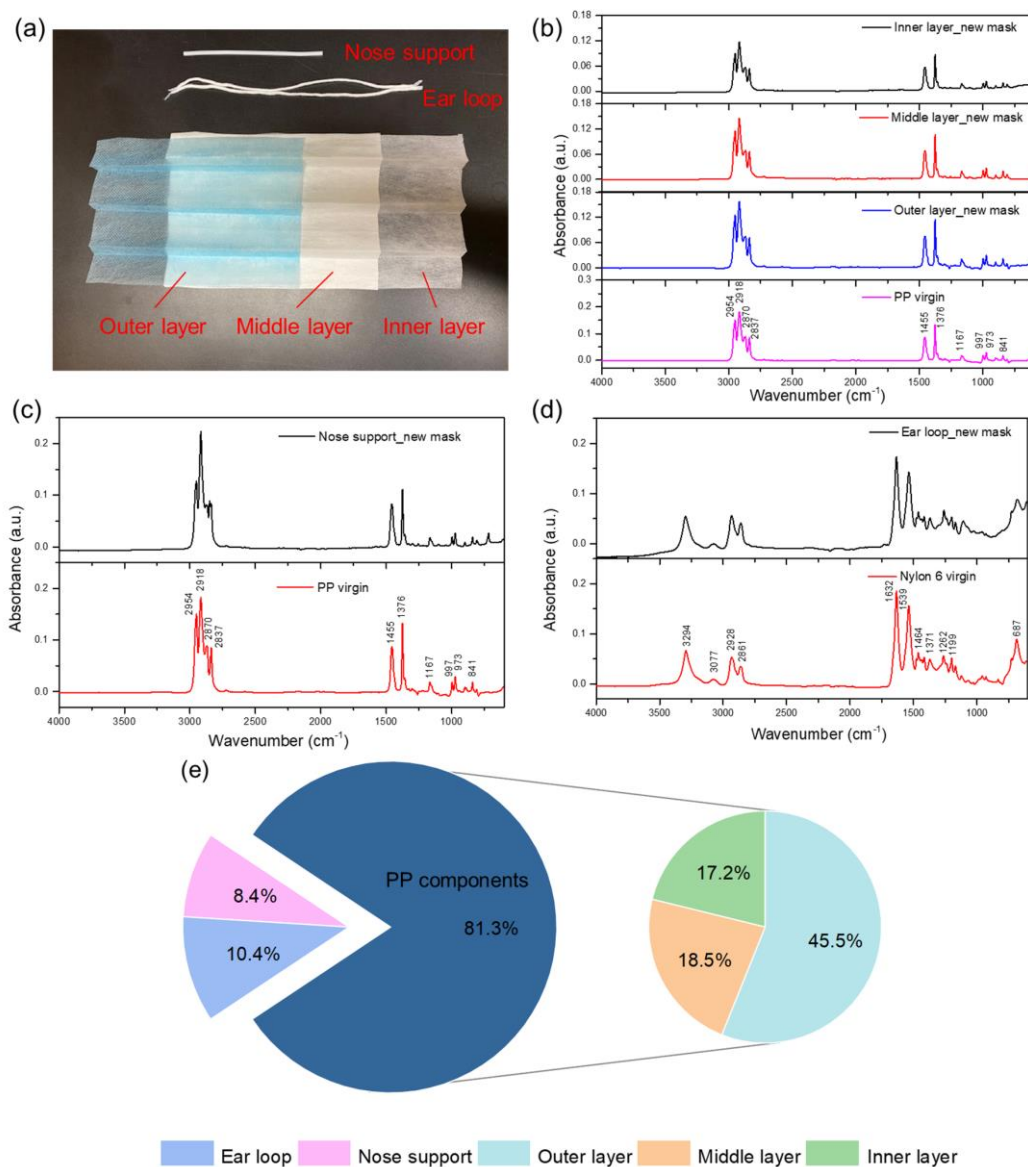


Figure 2. (a) Different components of disposable face masks. (b-d) ATR-FTIR spectra of each component from disposable face masks with virgin resin as reference. (e) Weight percentage of each component.

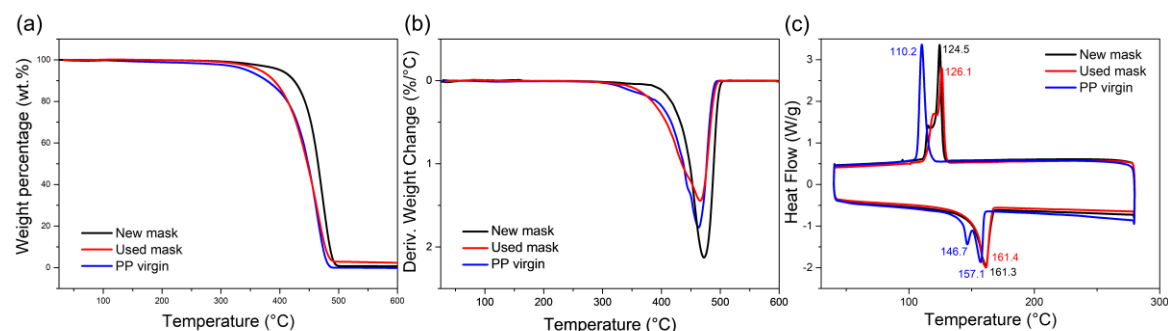


Figure 3. (a) TGA and (b) DTG (Derivative Thermogravimetry) curves of new mask, used mask and PP (ramping rate: 10°C/min, nitrogen flow rate: 50.0 mL/min). (c) DSC thermograms of new mask, used mask and PP (ramping rate: 10°C/min, nitrogen flow rate: 50.0 mL/min).



Table 1. Melting temperatures, heat of melting, crystallization temperature, and heat of crystallization for new mask, used mask, and PP.

Sample	$T_m$ (°C)	$\Delta H_m$ (J/g)	$T_c$ (°C)	$\Delta H_c$ (J/g)
New mask	161.3	90.57	124.5	102.50
Used mask	161.4	95.09	126.1	106.00
PP virgin	146.7/157.1	82.36	110.2	90.16

Figure 3 shows the TGA and DSC thermograms of the new mask, used mask, and virgin PP. The degradation temperatures ( $T_{d5\%}$ ) of new and used masks, and virgin PP in Figure 3a are 402°C, 366°C and 345°C. Here,  $T_{d5\%}$  represents the temperature at which 5% weight loss is observed. Even though the  $T_{d5\%}$  of the new mask was higher than the used mask and virgin PP, their main decomposition ranges were similar, from 320°C to 500°C.<sup>5,6</sup> The residual mass of used mask (2.85 wt-%) was slightly higher than that of virgin PP (0.02 wt-%), owing to the existence of inorganic compounds (e.g., white pigment) in the face mask. The main degradation phases of new mask, used mask, and virgin PP were centered at 472°C, 466°C, and 463°C, respectively (Figure 3b), indicating an insignificant change in thermal stability. Table 1 summarized the DSC results from Figure 3c at the second heating cycle. The double endothermic peaks at 146.7°C and 157.1°C were detected in virgin PP, which were the characteristic curves in the low molecular weight PP.<sup>24</sup> New and used masks showed similar DSC curves and their melting and crystallization temperatures were consistent. Cecon et al. characterized polyethylene (PE) and PET resins recovered using the STRAP process and observed that changes in the melting temperature were only noticeable when there was solvent retention in the polymer matrix.<sup>25</sup>

### 3.2 Polymer extraction via STRAP process

Toluene was used as the solvent to separate PP from the other polymers. We first evaluated the relationship between the yield of PP recovery and temperature. As shown in Figure S1, the PP recovery yield increases obviously with higher temperature. This experimental result is consistent with our recent work, in which the predicted solubility of PE, another type of polyolefins, could increase with elevating temperature.<sup>9</sup> Thus, in the following experiments, we used the boiling point of toluene (110°C) as the dissolution temperature. Tables 2 and S1 show the PP yield and undissolved fraction yield at different dissolution times. The overall yields are plotted in Figure S2. Five minutes of dissolution time removed the PP with ~73 wt-% recovery for new masks and ~72 wt-% for used masks. At the different dissolution times, the PP yields varied in the range of 72-76 wt-% for new mask and 71-74 wt-% for used mask. The yields of used mask were slightly lower than those of new mask. One possible reason was the

mixed manufacturers could result in the variable PP proportion. Furthermore, ATR-FTIR spectra (Figure 4a-b) exhibited that all recovered PP from different reaction times were identical to the virgin PP without any additional peaks observed. Figure S3a-b also show ATR-FTIR spectra of undissolved fractions at different dissolution times for new and used masks. The peaks attributed to nylon 6 and residual PP are clearly evident.

The weight average ( $M_w$ ) and number average ( $M_n$ ) molecular weights of the PP at different dissolution times were measured by HT-GPC as shown in Figure 5a-b. The polydispersity index (PDI) was presented to exhibit the molecular weight distribution (MWD).<sup>26</sup> The  $M_n$  for the new masks ranged from 46,335 to 76,452. This  $M_n$  for the used masks ranged from 35,690 to 54,436 which is slightly lower than for the new masks. The  $M_w$  for the new masks (102,330 to 139,310) was also higher than the  $M_w$  for the used masks (88,975 to 107,660). The PDI for the new masks ranged from 1.82 to 2.29, while the PDI for the used facemasks was slightly higher ranging from 1.89 to 2.49. These differences in molecular weight are likely because of differences in the starting values of the PP from different manufacturers.

Some changes are observed with molecular weight and PDI with time. However, there is no apparent trend for the molecular weight change at different dissolution times for new and used mask. K. F. Drain et al.<sup>27</sup> claimed that the PP did not degrade when refluxed in tetrachloroethylene at 121°C from 1 hour to 12 hours due to the relatively low boiling point solvent. In this paper we used a temperature of 110°C with reflux in toluene which is lower than what Drain et al. used. This suggests that it is unlikely that the PP degrades under the reaction conditions used in this study. The changes in molecular weight and PDI are likely due to different fractions of the PP being dissolved. Considering the used mask was close to the real waste and 5 min dissolution time was efficient to recover the majority of PP, thus, only used face masks were examined in the subsequent experiments and 5 min of dissolution time was used for the STRAP TEA. We attempted to measure melt flow rate (MFR) but couldn't get results, because our instrument was not an automatic equipment that was capable of running procedure B of the ASTM D1238.

Table 2. Yields of recovered PP from new and used mask.

<b>Dissolution time (min)</b>	<b>New mask recovery yield (%)</b>	<b>Used mask recovery yield (%)</b>
5	74.84 ± 0.84 <sup>ac</sup>	72.37 ± 1.04 <sup>ab</sup>
10	73.46 ± 0.52 <sup>ab</sup>	73.63 ± 0.58 <sup>b</sup>
30	72.40 ± 0.71 <sup>b</sup>	71.76 ± 0.39 <sup>a</sup>
60	75.80 ± 0.80 <sup>c</sup>	73.53 ± 0.86 <sup>ab</sup>

Same letters in the same column indicate statistical insignificance by Duncan's multiple range test.

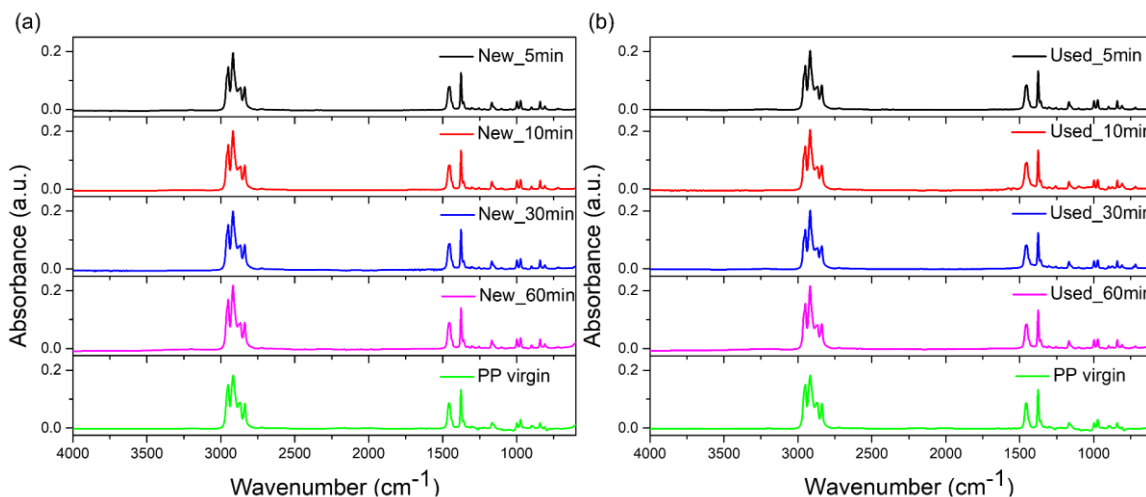


Figure 4. ATR-FTIR spectra of the recovered PP at different dissolution times conditions from (a) new mask and (b) used mask.

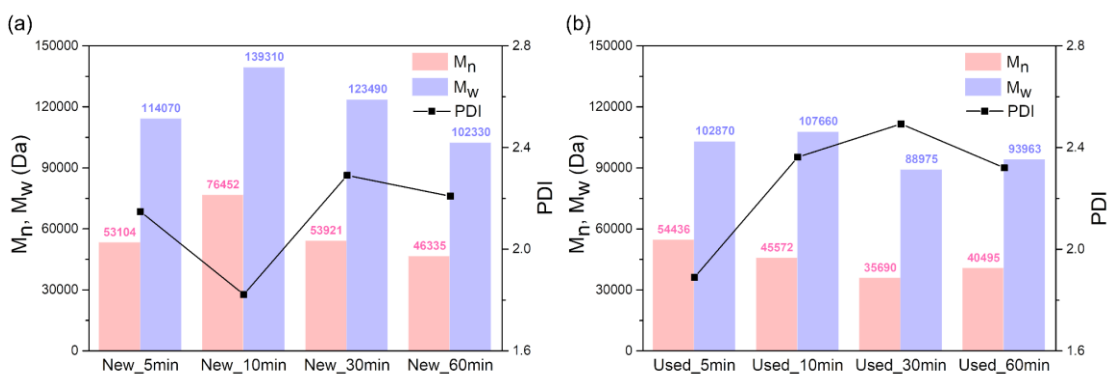


Figure 5. Weight average molecular weight ( $M_w$ ), number average molecular weight ( $M_n$ ), and polydispersity index (PDI) of recovered PP at different dissolution times, extracted from (a) new mask and (b) used mask.

### 3.3 Color removal process

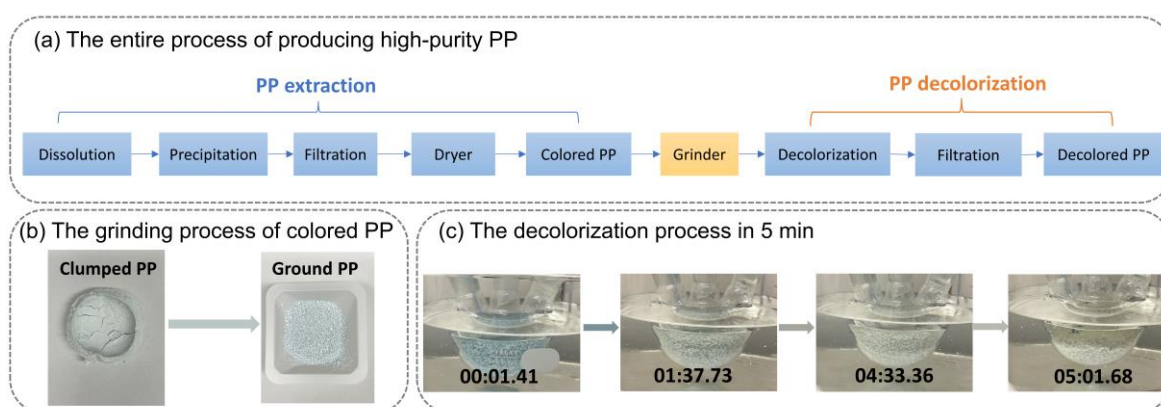


Figure 6. (a) The process to obtain high-purity PP, which includes extraction and decolorization steps. (b) Digital photos of clumped and ground PP. (c) Digital photos of decolorization process of extracted PP.

The full process to produce high-purity PP is displayed in Figure 6a. The extracted PP from the STRAP process had a light blue color, as shown in Figure 6b. Initially, acetone, isopropyl alcohol, dodecane, sodium hydroxide solution, and hexadecyltrimethylammonium bromide were chosen as screen test solvents, but no apparent color change was observed.<sup>28,29</sup> DMAc was ultimately selected as a decoloring solvent. However, due to the formation of clumped PP in the extraction process, DMAc did not completely adsorb to the PP and could not completely remove the color. A grinding process was then added following the extraction process to increase the contact area between PP and DMAc, as well as accelerate its decoloring rate. The clumped PP was ground to 3 mm in diameter (Figure 6b) using a milling machine before the decolorization step. DMAc was pre-heated at 115°C and then ground PP was added to the solvent (the mass ratio of ground PP : DMAc=1:15). The color of PP was removed in 5 min; detailed color changes are shown in the digital photos for the different extraction times (Figure 6c). To verify the completeness of color removal, we also examined a longer (60 min) decolorization experiment as the control test.

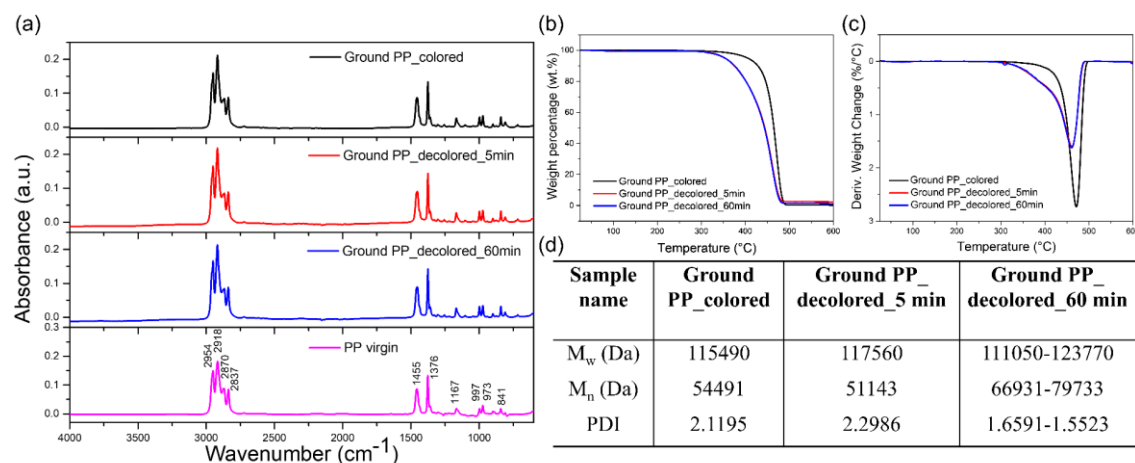


Figure 7. (a) ATR-FTIR spectra of ground PP without and with decolorization process. (b) TGA and (c) DTG curves of ground PP without and with the decolorization process (ramping rate: 10°C/min, nitrogen flow rate: 50.0 mL/min). (d) Results from HT-GPC of ground PP without and with decolorization process.

The characterization results of ground PP before and after the decolorization step are shown in Figure 7. From ATR-FTIR spectra (Figure 7a), all peaks of ground PP (colored or decolorized samples) were from virgin PP, implying a similar chemical structure as the virgin polymer. The colored PP and decolorized PP had slightly different decomposition temperatures (Figure 7b). Decomposition of the colored PP started at 335°C, which was very similar to the new or used face mask in Figure 3a. The decolorized PP began to decompose earlier at ~300°C. The main degradation phase of decolorized PP was at 460°C, while colored PP had a slightly higher degradation peak located at 470°C (Figure 7c). The molecular weight distribution results were listed in Figure 7d. With the addition of the decolorization process, the PDI of decolorized PP for 5 min did not change.

However, the PDI decreased with a longer extraction time. This decrease could be due to oxidized PP might have formed during processing.

ICP-OES was used to measure the metal concentration in the ground PP (extracted PP from used mask) before and after decolorization. Al and Fe were measured as they could potentially be in the nose piece. Common blue pigments include phthalocyanine blue ( $C_{32}H_{16}CuN_8$ ),<sup>30</sup> Prussian blue ( $Fe_7(CN)_{18} \cdot 14H_2O$ ),<sup>31</sup> C. I. Pigment Blue 36 ( $Al_2O_3 \cdot Cr_2O_3 \cdot CoO$ ), etc. Titanium dioxide is commonly used as the white pigment, and titanium tetrachloride is a common part of the polymerization catalyst for PP, so the Ti content was measured as well. As shown in Table 3, the Cr and Ni concentrations were very low in all PP samples. The Al and Fe concentrations were similar in all samples. However, the Cu concentration decreased by ~74% in the decolored PP. The increase of Ti concentration might be variation in the amount of  $TiO_2$  that snuck through the toluene extraction. Based on the effective removal of Cu in Table 3, phthalocyanine blue is likely used as the pigment.

Table 3. ICP-OES results of ground PP without and with decolorization process.

Sample name	Al (ppm)	Cr (ppm)	Cu (ppm)	Fe (ppm)	Ni (ppm)	Ti (ppm)
Ground PP_colored	137.72	*a	14.89	34.98	*b	65.32
Ground PP_decoded_5min	126.71	*b	3.94	34.47	*b	109.02
Ground PP_decoded_60min	125.42	*b	4.01	31.05	*b	86.17
Method LOD (ppm)	4.00	0.97	0.30	1.77	1.20	0.63
Method LOQ (ppm)	13.33	3.22	1.00	5.89	4.00	2.11

\*a: value between LOD and LOQ

\*b: value below LOD

The  $^1H$  and  $^{13}C$  spectra of virgin PP and decolored PP were analyzed by high-temperature NMR in solvent 1,1,2,2-tetrachloroethane- $d_2$ , as shown in Figure S4. All spectra were collected at 120°C, which was consistent with other reported literature.<sup>18</sup> Ten  $\mu L$  toluene was added as the internal standard. Both  $^1H$  and  $^{13}C$  spectra of decolored PP were consistent with the spectra of virgin PP, as well as in agreement with the literature.<sup>17</sup> In Figure S4b, three major signals at  $\delta$  46.0, 28.4, 21.4 ppm in  $^{13}C$  spectra

of virgin PP corresponded to the carbon of methylene, methine, and methyl groups in the PP chain.<sup>19</sup> The peak at  $\delta$  21.1 ppm was the methyl group of toluene.<sup>20</sup> In the decolored PP spectrum, the integrated ratio of methylene, methine and methyl groups was 1:1:1, indicating the typical characteristics of PP.

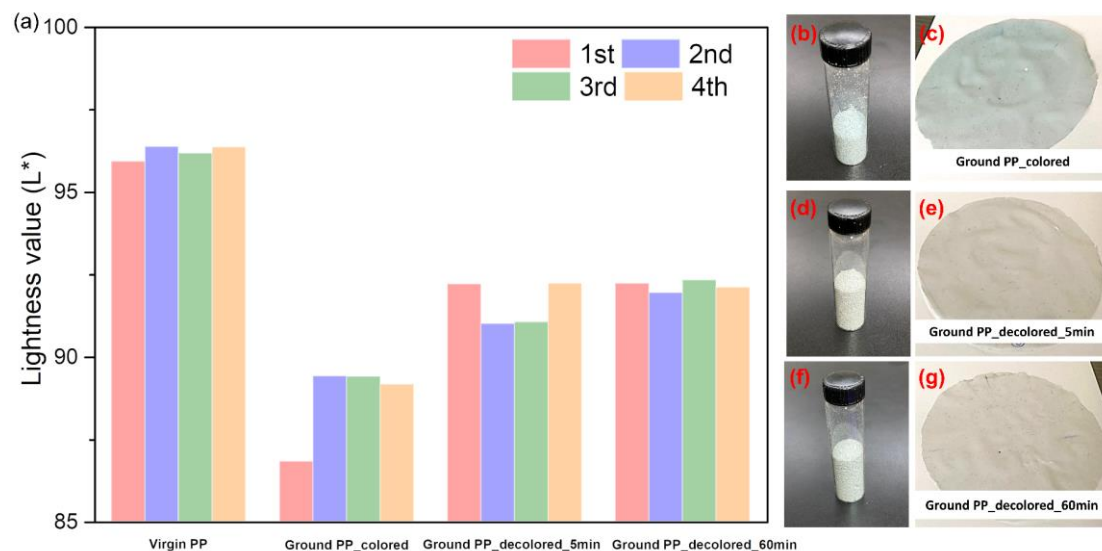


Figure 8. (a) Color quantification results for ground PP without and with decolorization process, using virgin PP as a control sample. Each sample was tested 4 times as shown by the different colors. Digital photos of powder samples and corresponding films after pressing: (b, c) ground PP\_colored; (d, e) ground PP\_decolorized\_5min; (f, g) ground PP\_decolorized\_60min.

Color quantification results were obtained based on the CIELAB color space, where L\* represented perceived lightness (perfect white = 100).<sup>16</sup> More detailed information can be found in Supporting Information (Table S2). In Figure 8a, virgin PP had the highest lightness, while the ground PP\_colored sample exhibited the lowest lightness value. Owing to the light color of colored PP, the difference between virgin and colored PP was not distinct. However, a positive improvement could still be detected in both decolored samples after the decolorization process.<sup>32</sup> In comparison, the lightness of 60 min decolorization time was similar to that of 5 min. The effectiveness of color removal could be visually verified in the photos, as shown in Figures 8b-g. Therefore, a high-purity PP was produced from face masks via STRAP technology. It should be noted that we recognize the limitations that might be imposed by the use of DMAc and our future work will focus on screening another suitable approach to remove the color.

### 3.4 Economic and environmental impacts of the PP extraction via STRAP process

#### 3.4.1 Technoeconomic analysis

We performed a TEA based on the collected experimental data of the process to analyze its economic feasibility. Figure 9 shows the process flow diagram indicating the main

equipment units and the input (face masks and toluene) and output (polypropylene) streams. Here, we can see the general steps of the process. First, the face masks are shredded, then, this stream and the toluene stream are heated and mixed in the dissolution vessel. This mixture is filtered and cooled down before going to the precipitation vessel. After this vessel, the mixture is filtered again. The liquid toluene stream is recycled and the other stream comprising PP and toluene is sent to a dryer to evaporate the residual toluene, producing a solid stream of PP and a gas stream of toluene. The toluene vapor is condensed, and the resulting liquid stream of cold toluene is used as a cooling agent in the heat exchanger to reduce utilities costs. The toluene stream is also recycled. The solid PP stream is ground to start the decolorization part of the process. Then, it is mixed with DMAc, heated, and sent to the dissolution vessel. This mixture is filtered; one part is sent to the dryer and condenser, while a fraction of the other part (10 wt-%) is sent to the distillation column. The remaining solvent is directly recycled along with the DMAc recovered from distillation and the condenser. Finally, the decolored PP is sent to the repelletizing extruder and storage tank.

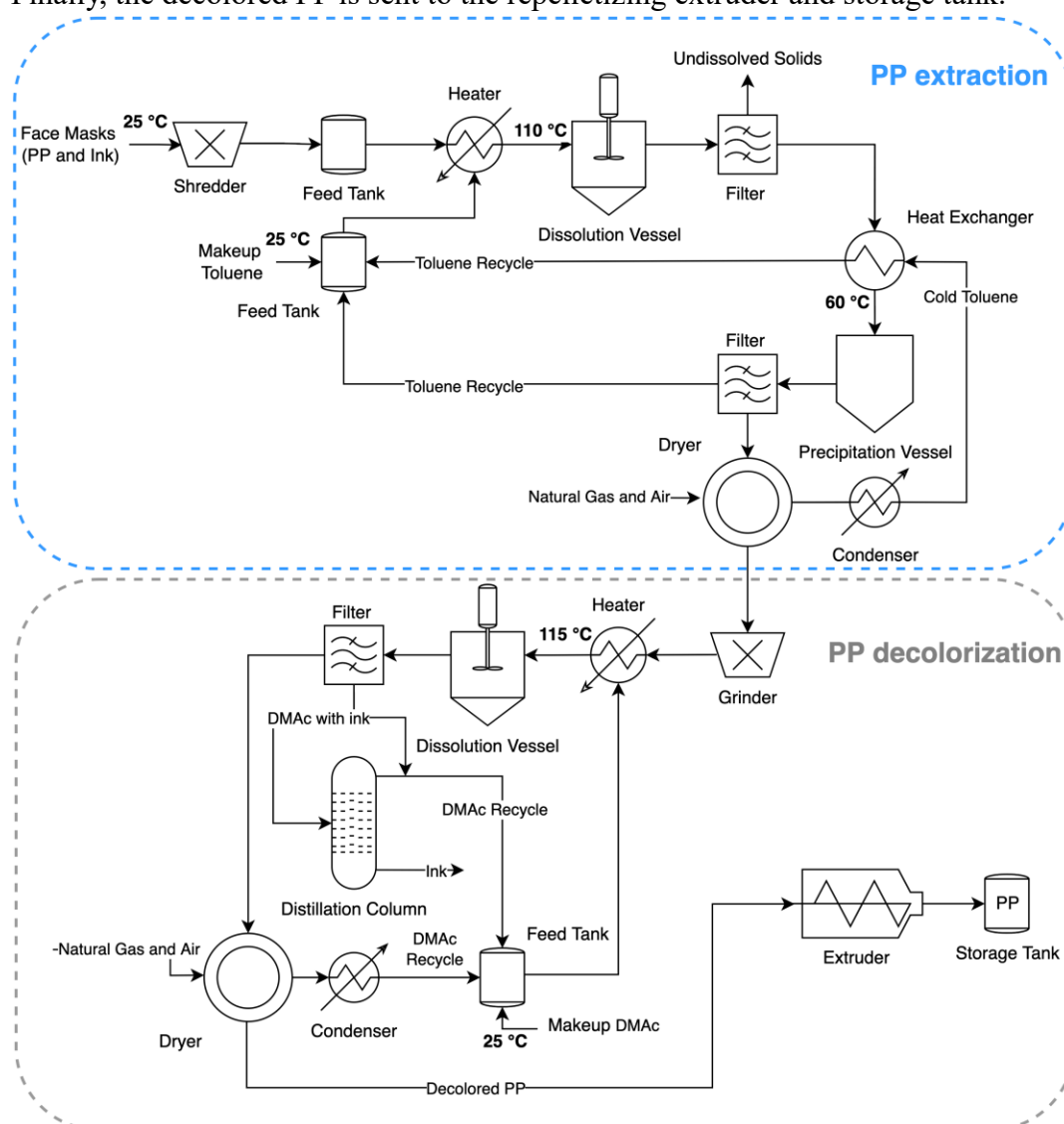


Figure 9. Process flow diagram for the recovery of the PP in face masks using the STRAP technology.

Mass and energy balances are used to estimate the capital and operating costs of the process. We calculated the minimum selling price (MSP) of the PP for a plant capacity of 5,292 tons per year. Our baseline analysis assumes that one recycling facility can obtain 50% of the face masks discarded from the population of Wisconsin. Some assumptions of the TEA include that the economic lifetime of the plant is 20 years, the interest rate is 10%, and the input stream of face masks does not have any cost since it is a waste (the transportation cost is not included either). The complete assumptions and parameters can be found in the Supporting Information (Table S3). To investigate the purity of recycled solvents, multiple techniques, including ATR-FTIR, high performance liquid chromatography (HPLC), and gas chromatography-mass spectrometry (GC-MS) were used to analyze the recycled toluene and distilled DMAc (Figures S5-7). From ATR-FTIR spectra (Figure S5), both recycled toluene and distilled DMAc were identical with the fresh solvent. To improve the accuracy of purity analysis, solvents were further analyzed by HPLC. As shown in Figure S6, both recycled toluene and distilled DMAc showed consistent HPLC profiles with the fresh solvents. GC-MS was used to identify trace elements in the samples. Figure S7a shows the solvents before and after STRAP. A new unidentified peak is observed in the toluene at 12.58 min which has 1.09% area percentage. This peak was not identified in our GC-MS database. No additional peak was observed from DMAc after the STRAP. More work is required to understand how often the solvents would need to be purified in a STRAP process. Our process simulation indicates a 99.97% of solvent recovery for the toluene and 99.98% for the DMAc is possible. For the processing capacity of 5,292 tons per year, we found that the MSP of the PP is 1.86 USD/kg. This price is comparable to the average market values of PP and the price of post-consumer PP (0.94-2.52 USD/kg).<sup>33, 34</sup> The total capital investment is 32.2 million USD, and the operating cost is 2.45 million USD per year. The detailed capital and operating costs are reported in Tables S4-S8 of the Supporting Information. The extruder and dryers are the equipment units that represent most of the capital cost (Table S4). This is consistent with our previous analysis.<sup>10</sup> Regarding the dryers, their contribution to the cost of this new STRAP process is related to the amount of solvent *trapped* in the PP. On the other hand, electricity, natural gas, and cooling agents are the utilities that contribute the most to the variable operating costs (Table S7). The detailed stream list and mass balance for the process can be found in Figure S8 and Table S9.

Figure 10 shows a sensitivity analysis for the selected parameters. We estimated the MSP when the value of these parameters increased or decreased by 30%. We can see that the MSP is sensitive to the interest rate.



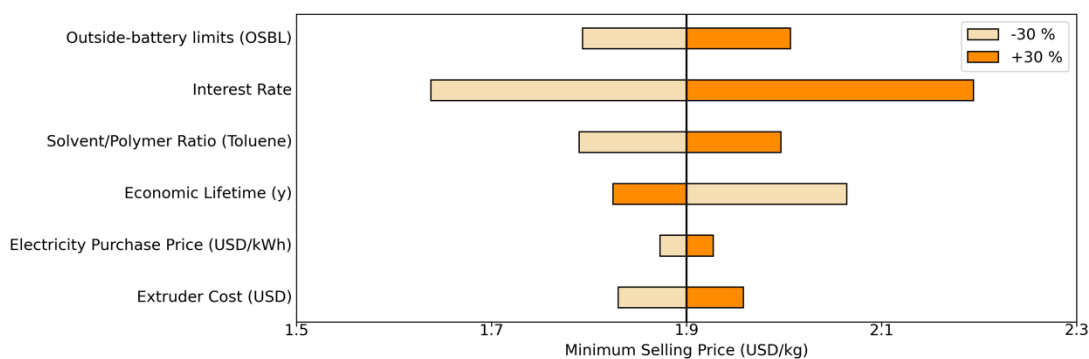


Figure 10. Sensitivity analysis for important parameters of the process.

We also performed a sensitivity analysis for different processing capacities to evaluate the impact of the economies of scale on the process. These results are presented in Figure 11. We observe that after 15,000 tons per year, the MSP of the PP produced in the STRAP process is around half the maximum market value of the virgin resin and the price of post-consumer PP (0.94-2.52 USD/kg).<sup>33, 34</sup> These results demonstrate that the STRAP process is economically viable and that this technology could be installed at a large scale to recover the PP in face mask waste.

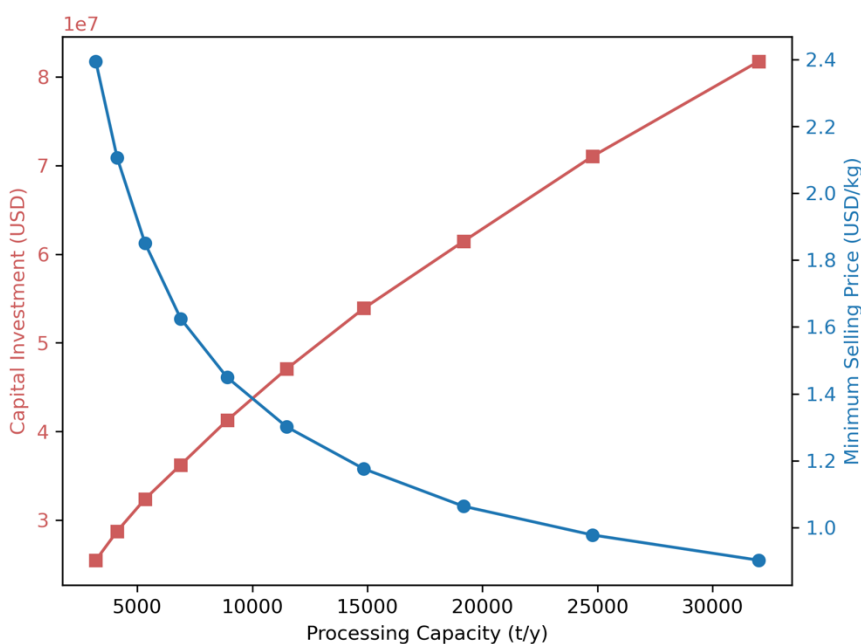


Figure 11. Sensitivity analysis for economies of scale.

The TEA for the polymer extraction via the STRAP technology without the color removal process is presented in the Supporting Information section. Here, we found that the MSP of the recovered PP without color removal is 1.42 USD/kg.

### 3.4.2 Environmental impact analysis

We analyzed the impacts of STRAP on climate change (kg CO<sub>2</sub> eq.) using a LCA methodology from a product perspective.<sup>35</sup> From this perspective, the STRAP approach

is seen as an alternative process to the production of high-purity PP. The functional unit considered is the production of 1 kg of PP. Therefore, we compare the environmental impacts of producing 1 kg of PP from traditional pathways with producing 1 kg of PP through the STRAP process. In Figure 12, we can see that the total impacts of the STRAP process (0.87 kg CO<sub>2</sub> eq./kg PP) are lower than the impacts of the virgin resin production (2.07 kg CO<sub>2</sub> eq./kg PP). Specifically, around 58% less emissions are generated in the STRAP process. We can see that most of the emissions in the STRAP process are related to the use of electricity and steam. Due to the data available in the LCA databases used for this study (see Supporting Information), electricity and steam impacts are modeled based on the following mix. For electricity, the mix includes 78% of non-renewable energy sources, while for steam, the mix involves 87.5% of non-renewable energy sources. Therefore, it is worth highlighting that, if electricity and steam were produced from more or only renewable sources, the environmental impacts would be much lower. We find that the STRAP process can help achieve the goals of a circular economy by reducing resource consumption and environmental impacts.

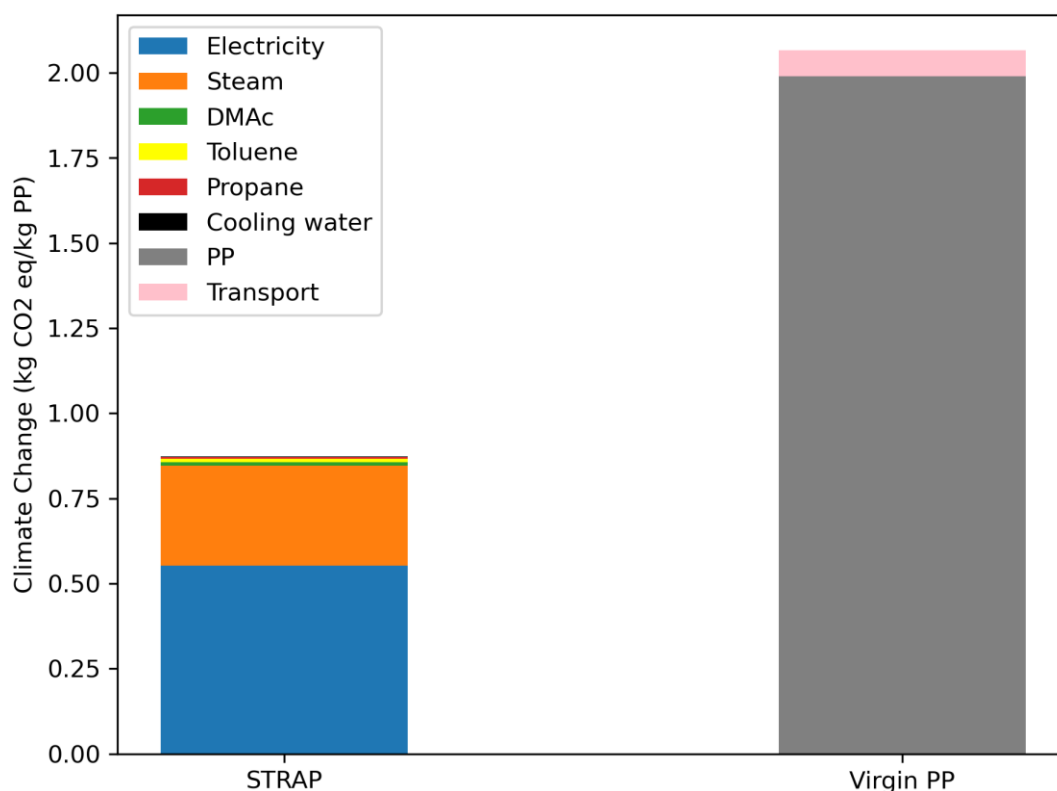


Figure 12. Climate change impact of producing high-purity PP via the STRAP process in comparison with virgin PP.

The environmental impact of the polymer extraction via the STRAP technology without the color removal process and more details about the LCA methodology are presented in the Supporting Information. We found that around 72% fewer emissions are generated in the STRAP process to recover PP with color.

## 4. Conclusions

In this work, the solvent-targeted recovery and precipitation (STRAP) technology was applied to recover PP from disposable face masks. Nearly 90 wt-% of PP was extracted and separated with a dissolution time of less than 5 min. The recovered PP was chemically comparable to virgin resin but still had a blue color. A decolorization step with DMAc was subsequently applied to the extracted PP and high-quality PP was recovered. The decolored PP had similar thermo- and chemical properties to the virgin PP. The TEA indicated that the STRAP process could produce high-purity PP at a comparable price to the average market value of the virgin resin and the price of post-consumer PP for processing capacities greater than 5,000 tons per year. Environmental impact analysis also supports the reduction of resource consumption by replacing virgin PP production with PP recovered using STRAP technology.

These results demonstrate that the STRAP process is economically feasible, and this technology could be installed at a large scale to recover PP from face mask waste. The TEA shows that the equipment units that represent most of the costs are the extruder, the dryers, and the condenser. This occurs because of the type of solvent used, the type of polymer (polypropylene), which leads to solvent retention (there is solvent trapped in the polymer). Additionally, the ratio between the polymer and the solvent is a parameter that highly impacts the cost of the process. Our future work will focus on the improvement and modification of PP recycling process with lower cost and a simplified procedure.

## 5. Author contributions

Jiuling Yu: Conceptualization, Methodology, Validation, Formal analysis, Investigation, Writing - Original draft, Visualization; Aurora del Carmen Munguía-López: Methodology, Software, Formal analysis, Writing - Original draft; Victor S. Cecon: Investigation, Writing - Review & Editing; Kevin L. Sánchez-Rivera: Methodology, Writing - Review & Editing; Kevin Nelson: Methodology, Writing - Review & Editing; Jiayang Wu: Investigation, Writing - Review & Editing; Shreyas Kolapkar: Writing - Review & Editing; Victor M. Zavala: Writing - Review & Editing; Greg W. Curtzwiler: Writing - Review & Editing; Keith L. Vorst: Writing - Review & Editing; Ezra Bar-Ziv: Writing - Review & Editing; George W. Huber: Resources, Writing - Review & Editing, Supervision, Funding acquisition.

## 6. Acknowledgements

This work was performed through the Chemical Upcycling of Waste Plastics (CUWP) center, which is supported by the U.S. Department of Energy (DOE), Office of Energy Efficiency and Renewable Energy, and Bioenergy Technologies Office under Award Number DEEE0009285. The authors acknowledge Professor Ive Hermans for providing an ATR-FTIR for us to use. Jiuling Yu would like to thank Feng Cheng,

Panzheng Zhou, Javier Chavarrio-Cañas, Hoya Ihara, Shao-Chun Wang, and Stas Zinchik for their help on discussions about characterizations, solvent selection, equipment set-up and sample preparation.

## 7. References

1. J. C. Prata, A. L. Silva, T. R. Walker, A. C. Duarte and T. Rocha-Santos, *Environmental Science & Technology*, 2020, **54**, 7760-7765.
2. O. F. LTD, COVID-19 facemasks & marine plastic pollution, <https://oceansasia.org/covid-19-facemasks>.
3. K. Selvaranjan, S. Navaratnam, P. Rajeev and N. Ravintherakumaran, *Environmental Challenges*, 2021, **3**, 100039.
4. M. Xiang, Z. Yang, S. Zhou, T. Lu, S. Zhang, L. Sun and S. Dong, *ACS Applied Polymer Materials*, 2021, **3**, 3679-3684.
5. S. Jung, S. Lee, X. Dou and E. E. Kwon, *Chemical Engineering Journal*, 2021, **405**, 126658.
6. D. Battegazzore, F. Cravero and A. Frache, *Resources, Conservation and Recycling*, 2022, **177**, 105974.
7. D. J. Muensterman, L. Cahuas, I. A. Titaley, C. Schmokel, F. B. De la Cruz, M. A. Barlaz, C. C. Carignan, G. F. Peaslee and J. A. Field, *Environmental Science & Technology Letters*, 2022, **9**, 320-326.
8. R. Yu, X. Wen, J. Liu, Y. Wang, X. Chen, K. Wenelska, E. Mijowska and T. Tang, *Applied Catalysis B: Environmental*, 2021, **298**, 120544.
9. T. W. Walker, N. Frelka, Z. Shen, A. K. Chew, J. Banick, S. Grey, M. S. Kim, J. A. Dumesic, R. C. Van Lehn and G. W. Huber, *Science Advances*, 2020, **6**, eaba7599.
10. K. L. Sánchez-Rivera, P. Zhou, M. S. Kim, L. D. González Chávez, S. Grey, K. Nelson, S. C. Wang, I. Hermans, V. M. Zavala, R. C. Van Lehn and G. W. Huber, *ChemSusChem*, 2021, **14**, 4317-4329.
11. P. Zhou, J. Yu, K. L. Sánchez-Rivera, G. W. Huber and R. C. Van Lehn, *Green Chemistry*, 2023, **Accepted**.
12. L. Ye, X. Zhao, E. Bao, J. Li, Z. Zou and K. Cao, *Scientific Reports*, 2020, **10**, 1-11.
13. F. Cheng, Z. Cui, K. Mallick, N. Nirmalakhandan and C. E. Brewer, *Bioresource Technology*, 2018, **258**, 158-167.
14. A. International, *ASTM D6474-20. Standard test method for determining molecular weight distribution and molecular weight averages of polyolefins by high temperature gel permeation chromatography*, West Conshohocken, PA, USA, 2020.
15. V. S. Cecon, P. F. Da Silva, K. L. Vorst and G. W. Curtzwiler, *Polymer Degradation and Stability*, 2021, **190**, 109627.
16. T. D. Lillotte, M. Joester, B. Frindt, A. Berghaus, R. F. Lammens and K. G. Wagner, *International Journal of Pharmaceutics*, 2021, **603**, 120668.
17. M. Zhang, J. Liu, Y. Wang, L. An, M. D. Guiver and N. Li, *Journal of Materials*

- Chemistry A*, 2015, **3**, 12284-12296.
18. P. Chammingkwan, F. Yamaguchi, M. Terano and T. Taniike, *Polymer Degradation and Stability*, 2017, **143**, 253-258.
  19. M. Scoti, F. De Stefano, R. Di Girolamo, A. Malafronte, G. Talarico and C. De Rosa, *Macromolecular Chemistry and Physics*, 2023, **224**, 2200262.
  20. J. Zakzeski, S. Burton, A. Behn, M. Head-Gordon and A. T. Bell, *Physical Chemistry Chemical Physics*, 2009, **11**, 9903-9911.
  21. M. Jung, Y. Lee, S. Kwak, H. Park, B. Kim, S. Kim, K. H. Lee, H. S. Cho and K. Y. Hwang, *Analytical Chemistry*, 2016, **88**, 1516-1520.
  22. H. Chang, E. B. Gilcher, G. W. Huber and J. A. Dumesic, *Green Chemistry*, 2021, **23**, 4355-4364.
  23. Y. Cortes-Peña, D. Kumar, V. Singh and J. S. Guest, *ACS Sustainable Chemistry & Engineering*, 2020, **8**, 3302-3310.
  24. R. Paukkeri and A. Lehtinen, *Polymer*, 1993, **34**, 4083-4088.
  25. V. S. Cecon, G. W. Curtzwiler and K. L. Vorst, *Macromolecular Materials and Engineering*, 2022, 2200346.
  26. L. W. McKeen, *The effect of sterilization on plastics and elastomers*, William Andrew, 2018.
  27. K. Drain, W. Murphy and M. Otterburn, *Conservation & Recycling*, 1983, **6**, 123-137.
  28. M. Soylu, Ö. Gökkuş and F. Özyonar, *Separation and Purification Technology*, 2020, **247**, 116985.
  29. K. Shakir, A. F. Elkafrawy, H. F. Ghoneimy, S. G. E. Beheir and M. Refaat, *Water Research*, 2010, **44**, 1449-1461.
  30. A. Ragusa, A. Svelato, C. Santacroce, P. Catalano, V. Notarstefano, O. Carnevali, F. Papa, M. C. A. Rongioletti, F. Baiocco and S. Draghi, *Environment International*, 2021, **146**, 106274.
  31. N. D. Nia, S.-W. Lee, S. Bae, T.-H. Kim and Y. Hwang, *Applied Surface Science*, 2022, **590**, 153101.
  32. Y. Yao, E. Chau and G. Azimi, *Waste Management*, 2019, **97**, 131-139.
  33. S. P. Global, *POLYMERSCAN. Americas polymer spot price assessments*, 2021.
  34. Statista, Price of polypropylene worldwide from 2017 to 2022, <https://www.statista.com/statistics/1171084/price-polypropylene-forecast-globally/#:~:text=In%202021%2C%20the%20average%20global,1%2C208%20U.S.%20dollars%20per%20ton>, (accessed Jun 16, 2022).
  35. H. Jeswani, C. Krüger, M. Russ, M. Horlacher, F. Antony, S. Hann and A. Azapagic, *Science of the Total Environment*, 2021, **769**, 144483.